THE JOURNAL OF PHYSICAL CHEMISTRY B LETTERS

2008, *112,* 2757−2760
Published on Web 02/15/2008

Carrier Relaxation Dynamics in Lead Sulfide Colloidal Quantum Dots

Emanuel Istrate,*,† Sjoerd Hoogland, Vlad Sukhovatkin, Larissa Levina, Stefan Myrskog, Peter W. E. Smith, and Edward H. Sargent

Department of Electrical and Computer Engineering, University of Toronto, 10 King's College Road, Toronto, Ontario, M5S 3G4, Canada

Received: August 24, 2007; In Final Form: December 17, 2007

We report transient absorption saturation measurements on lead sulfide colloidal nanocrystals at the first and second exciton energies and fit the results to a model incorporating intraband and interband relaxation processes. We study in detail the Auger recombination from the first excited state, which takes place when more than one electron−hole pair is excited in a dot. We find an Auger coefficient of 4.5×10^{-30} cm^6/s for dots of 5.5 nm diameter, and observe saturation of the absorption bleaching when the (8-fold degenerate) first level is filled. We develop a model for the absorption dynamics using Poisson statistics and find a good fit with our experimental measurements.

1. Introduction

Colloidal semiconductor nanocrystals[1] offer the versatility of semiconductors with simplified processing methods. Lead salt nanocrystals[2] have a band edge tunable from red to beyond the infrared telecommunications wavelength,[2,3] where no other practical solution-processable organic semiconductors exist. Many lead salt nanocrystal devices have been demonstrated, such as lasers,[4] photodetectors,[5] photovoltaic solar cells,[6,7] modulators,[8] and transistors.[9]

The delocalized carriers in bulk semiconductors lead to Auger processes proportional to the cube of the carrier density. In quantum dots, however, the strong confinement of excitons gives a sharp threshold for Auger processes. They are absent with only one exciton, but occur efficiently when additional excitons are available. Therefore, carrier relaxation rates differ by several orders of magnitude between dots with single and multiple excitons, as observed previously in several types of nanocrystals, including PbSe[10−12] and other II−VI semiconductors,[13,14] but PbS nanocrystals have not previously been studied.

Here we report the first detailed investigation of relaxation and recombination dynamics in PbS quantum dots, providing a model for their fundamental processes. Although absorption dynamics in PbS nanocrystals embedded in glasses[15] and other non-luminescent colloids[16] have been investigated before, we use the higher quality nanocrystals available today. Earlier studies[17] investigated absorption saturation at energies high above the band gap with no correlations to the electronic structure. We measure and model the Auger coefficient for relaxation from the fundamental exciton state and the carrier lifetime in the higher excited states. We explain the change in absorption at high pump intensities and the saturation of this change, and show experimentally that the degeneracy of the fundamental quantum dot level is 8.[18] Our nanocrystals have photoluminescence at the important telecommunications wavelength of 1550 nm.

Auger recombination has previously been modeled in other nanocrystals using Poisson distributions.[11] For PbS nanocrystals, we expand previous models by limiting the fundamental level occupancy to its degeneracy and are thus able to account for the observed saturation in the absorption change.

Auger processes speed up recombination but usually reduce luminescence. Thus they are useful for fast nonlinear optical devices, but should be avoided where long lifetimes or high luminescence efficiencies are required, for example, in multiple-exciton generation devices.[19] Therefore, a good understanding of multi-exciton recombination is needed for the design of many nanocrystal devices. Since nanocrystal electron dynamics are not completely understood, this study may also prove to be useful for devices in other materials systems.

2. Experimental Details

Our PbS nanocrystals[20] are capped with oleate ligands and dispersed in toluene. They have a diameter near 5.5 nm, and a fundamental exciton energy of 0.84 eV, with an absorption peak at 1480 nm. Their photoluminescence quantum efficiency is 24%, measured using an integrating sphere. The concentration as estimated from the mass left after evaporation of the solvent is 1.1×10^{13} dots/μL (8.5 μg/μL). We expect that the true density will, however, be lower because excess ligands in the solution will contribute to the measured mass.

Absorption transients are monitored in a pump−probe setup with 2 ps and 800 nm pump pulses, and 2 ps probe pulses tuned from 800 to 1600 nm, at a repetition rate of 1 kHz. The probe fluence is 3.5 μJ/cm^2. The pump fluence ranges from 80 to 5600 μJ/cm^2. The pump and the probe beams meet at an angle of 20° with spot sizes of 400 and 60 μm, respectively. The solution is in a cuvette with an internal path length of 1 mm. The pump and probe pulses overlap over the entire thickness of the cuvette.

The sample absorbs ∼40% of the pump fluence; ∼50% is transmitted, and the rest is reflected. No pump absorption

* Corresponding author. E-mail: e.istrate@utoronto.ca.
† Currently with the Institute for Optical Sciences, University of Toronto, 60 St. George Street, Toronto, Ontario, M5S 1A7, Canada.

10.1021/jp076809g CCC: $40.75

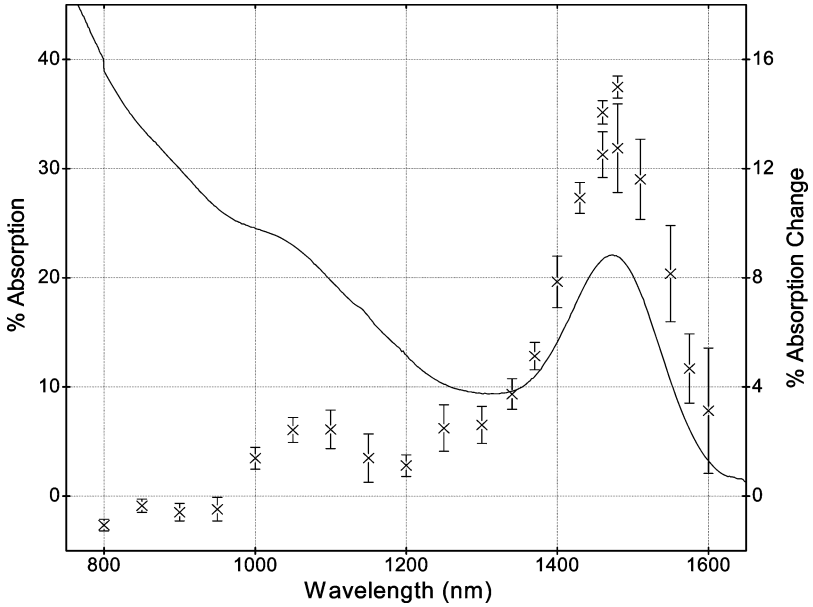

Figure 1. Linear absorption (line) and maximum absorption change (points) of the nanocrystals. The maximum absorption change occurs approximately 2 ps after the arrival of 4 mJ/cm^2 pump pulses. The pump wavelength is 800 nm.

saturation was observed. The pump does not produce boiling of the solution.

3. Results

The linear absorption, measured with a CARY 500 spectrometer, is shown in Figure 1 (solid line). The first two exciton peaks are visible. The change in absorption with 4 mJ/cm^2 pump pulses is also shown (points). It is strongest at the fundamental exciton energy, eliminating almost the entire linear absorption. Only very weak gain is observed at longer wavelengths, indicating that additional non-saturable or exited-state absorption mechanisms exist in such dots, as previously observed.[11]

The change in absorption is nearly zero between the first two excitons and increases again at the second exciton, indicating carrier accumulation. At shorter probe wavelengths, the absorption saturation becomes negative, indicating excited-state absorption.

Figure 2a shows the evolution of the absorption change, or bleaching, at the fundamental exciton (1480 nm), with pump fluences between 80 and 5600 μJ/cm^2. Figure 2b shows the dynamics at the second exciton (1050 nm), for fluences between 800 and 4000 μJ/cm^2. Maximum bleaching versus pump fluence is shown in Figure 3.

At the fundamental exciton wavelength, bleaching recovery depends strongly on pump levels. At high pump fluences, most of the bleaching recovers within 200 ps, but a slow component remains. The fast component is not exponential: recovery at early times is faster than that at later times, indicating a multi-exciton Auger process. No increase in bleaching is observed for fluences above 1200 μJ/cm^2, suggesting that, at this point, the 8-fold degenerate fundamental level[18] is filled. This is different from CdSe nanocrystals, where bleaching increases after the first exciton level is filled.[13] The strength of the long-time component is approximately 1/8 of the peak absorption change, consistent with the 8-fold degeneracy of the state. Its recovery, measured with a continuous wave probe laser and a fast photodetector, has a single-exponential decay with time constant of 500 ns.

The second exciton dynamics are different. The absorption saturation is 6 times weaker with an exponential decay of time

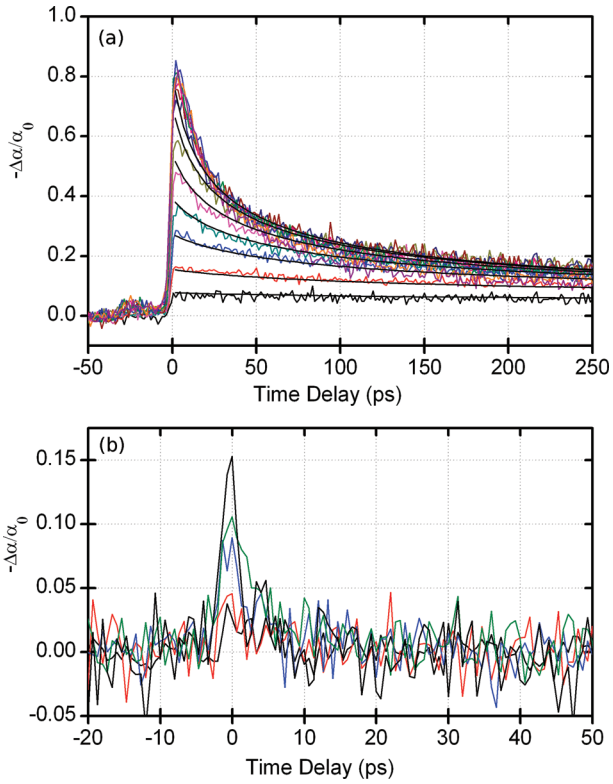

Figure 2. (a) Absorption saturation dynamics at the first exciton energy (1480 nm). From the bottom to the top, the pump fluences are 80, 160, 280, 400, 560, 800, 1200, 1600, 2000, 2400, 3200, 4000, and 5600 μJ/cm^2. The smooth lines represent fits using the Auger recombination model presented in Section 4. (b) Absorption saturation dynamics at the second exciton energy. The pump fluences are 800, 1600, 2400, 3200, and 4000 μJ/cm^2.

constant near 4 ps. There is no long-time component and no saturation in the bleaching amplitude for the pump fluences used here.

The bleaching rise times at the two wavelengths are single-exponential. At the second exciton, the time constants are near 1.5 ps, limited by the 2 ps laser pulses. At the first exciton, the rise time is near 3.5 ps. Nanocrystals in a solid film show the

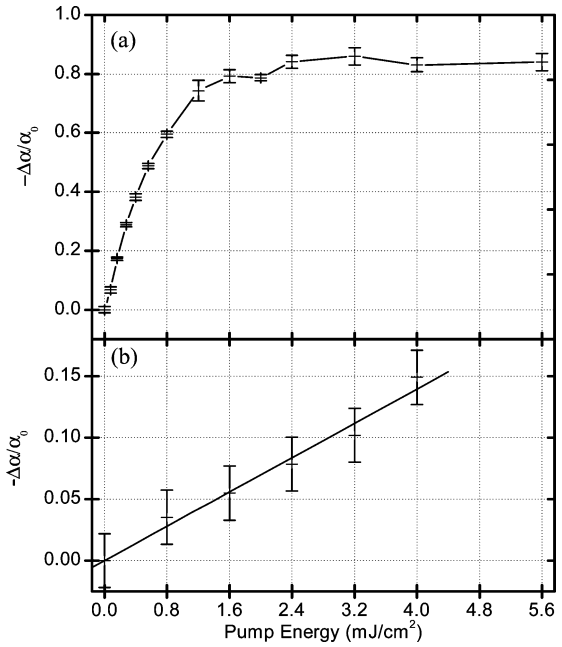

Figure 3. (a) Maximum absorption saturation as function of pump power at the wavelength of the first exciton. The error bars represent the standard deviation from four repeated measurements. (b) Maximum absorption saturation as a function of pump power at the second exciton wavelength.

same rapid recovery shown in Figure 2a, with similar rates. The slow component, however, is faster in the film (decay time near 15 ns), indicating that it depends on surface properties, while the fast Auger relaxation does not.

4. Modeling of Results

Auger recombination in nanocrystals depends on the total number of excitons per dot, since interdot interactions are unlikely at this time scale. As in bulk, it is a three-particle process, proportional to the carrier number cubed. It is impossible with a single exciton, resulting in the long lifetime component remaining at the end of the first 200 ps, when all dots with multiple excitons have relaxed to a single exciton.

The number of photons absorbed by each dot, producing high-energy excitons, is given by a Poisson distribution,[21] since no state-filling is observed at the pump wavelength. These excitons decay rapidly to the fundamental exciton. For low pump powers, the distribution of fundamental excitons is therefore described by the same Poisson statistic. At higher powers, however, the 8-fold degeneracy of the fundamental exciton will limit the occupancy at that level. If more than eight energetic excitons are created, the excess excitons recombine without entering this level. We justify this assumption with the identical bleaching recovery curves for 1200 and 5600 μJ/cm^2 pump fluences in Figure 2a, which imply that, in both cases, the same number of fundamental exciton states is occupied. We postulate that the excess excitons enter defect states in which they are not detectable by pump−probe measurements.

We therefore use a Poisson distribution for the population in the fundamental level, modified to limit the number of excitons to eight. We assume the recombination rate to be proportional to the number of excitons cubed, but to be zero for dots with one exciton. This assumption will be discussed later.

To illustrate these statistics, Figure 4 shows the initial (after intraband relaxation but before recombination) and final (after Auger recombination) distributions of fundamental excitons for dots that have absorbed an average of 1, 4, 8, and 12 photons.

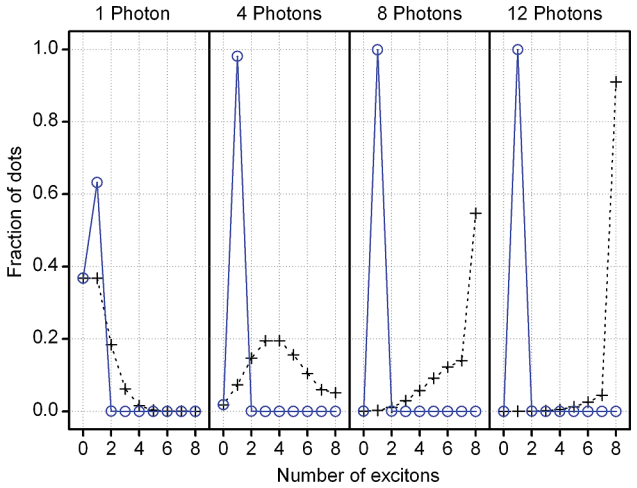

Figure 4. Initial (+) and final (○) distribution of excitons per dot for dot collections that have absorbed an average of 1, 4, 8, and 12 photons per dot, as described in the text. Lines are added for visibility.

For an average of one exciton, 24% of the dots have more than one exciton and can undergo Auger recombination. At an average of four excitons, only 2% of the dots are unexcited, which means that, after Auger recombination, almost all dots have one exciton. For stronger excitations, the slow component of absorption saturation will therefore not increase. For an average absorption of eight photons, only 55% of the dots receive eight fundamental excitons. Complete state filling and maximum absorption change is reached around an average absorption of 12 photons.

The evolution from the initial to the final distributions in Figure 4 obeys the following equations:

$$\frac{dP_n}{dt} = C_A[(n+1)^3 P_{n+1}],\ n = 1$$

$$\frac{dP_n}{dt} = C_A[-n^3 P_n + (n+1)^3 P_{n+1}],\ 2 \le n \le 7$$

$$\frac{dP_n}{dt} = C_A[-n^3 P_n],\ n = 8 \qquad (1)$$

where P_n is the proportion of dots with n fundamental excitons, and C_A is the Auger coefficient. n denotes the unitless number of excitons per dot. Using the data from Figure 2a (fits shown with smooth lines) results in an Auger coefficient $C_A = 590 \times 10^6$ s^{-1}. Pump fluences between 80 and 1200 μJ/cm^2 yield between 0.8 and 12 energetic excitons per dot. The fits in Figure 2a involve only two free parameters: the Auger coefficient C_A, and the correspondence between exciton density and pump fluence.

The density of dots, estimated in section 2 to be $<1.1 \times 10^{13}$ dots per μL, requires a fluence of <680 μJ/cm^2 for one exciton per dot. From the data in Figure 2a we obtain a fluence of $\sim$100 μJ/cm^2 for one exciton per dot. The discrepancy between these results is attributed to the excess ligands, which add to the measured mass. From the data fits, we obtain an absorption cross section at 800 nm of 2.5×10^{-15} cm^2.

We used an n^3 dependence for Auger recombination because three charge carriers are involved. To test this assumption, we tried to fit our data to an n^2 dependence. No good fit was obtained.

Using a nanocrystal volume of 87×10^{-21} cm^3, we can convert our Auger coefficient to the form used in bulk

semiconductors: $C = 4.5 \times 10^{-30}$ cm^6/s. This number is within an order of magnitude of the coefficient of bulk GaAs[22] and nanocrystalline CdSe[13] and is approximately 2 orders of magnitude lower than the coefficient of bulk PbSe[23,24] and PbTe.

At the second exciton, the fast, single-exponential bleaching recovery and the well-known lack of phonon bottleneck[10] indicate that excitons enter and leave this state rapidly on their way to the lowest level. The lack of bleaching saturation shows that the 16 degenerate states at this level[18] are not filled. We postulate that charge carriers that do not find a free state at the fundamental energy level enter defect states below the second exciton.

5. Conclusions

We investigated exciton dynamics at the first and second energy levels of PbS quantum dots and found that, if more than one fundamental exciton is excited per dot, Auger recombination takes place, with a rate proportional to the number of excitons cubed and a coefficient of 4.5×10^{-30} cm^6/s. For dots with a single exciton, recombination takes place through slower mechanisms with a time of 500 ns. The bleaching saturation indicates that the fundamental exciton is 8-fold degenerate. Once filled, additional excitons do not contribute to absorption saturation, in contrast with CdSe. The similarity in the decay curves for highly excited dots indicates that the first eight excitons relax to the fundamental level, and the others recombine without passing through that level.

Knowledge and control over the behavior of Auger processes is necessary for this material to be used efficiently in devices. Photovoltaic devices, photodetectors, and photoluminescent devices need long carrier lifetimes, and Auger processes must be minimized. High-speed signal processing devices, however, benefit from the rapid recovery provided by Auger recombination. In both cases, knowledge of Auger processes is an important first step in the design of devices.

References and Notes

(1) Alivisatos, A. P. *Science* **1996**, *271*, 933−937.
(2) Wise, F. W. *Acc. Chem. Res.* **2000**, *33*, 773−780.
(3) Hines, M. A.; Scholes, G. D. *Adv. Mater.* **2003**, *15*, 1844−1849.
(4) Hoogland, S.; Sukhovatkin, V.; Howard, I.; Cauchi, S.; Levina, L; Sargent, E. H. *Opt. Express* **2006**, *14*, 3273−3281.
(5) Konstantatos, G.; Howard, I.; Fischer, A.; Hoogland, S.; Clifford, J.; Klem, E.; Levina, L.; Sargent, E. H. *Nature* **2006**, *442*, 180−183.
(6) McDonald, S. A.; Konstantatos, G.; Zhang, S.; Cyr, P. W.; Klem, E. J. D.; Levina, L.; Sargent, E. H. *Nat. Mater.* **2005**, *4*, 138−142.
(7) Zhang, S.; Cyr, P. W.; McDonald, S. A.; Konstantatos, G.; Sargent, E. H. *Appl. Phys. Lett.* **2005**, *87*, 233101.
(8) Klem, E. J. D.; Levina, L.; Sargent, E. H. *Appl. Phys. Lett.* **2005**, *87*, 053101.
(9) Talapin, D. V.; Murray, C. B. *Science* **2005**, *310*, 86−89.
(10) Wehrenberg, B. L.; Wang, C.; Guyot-Sionnest, P. *J. Phys. Chem. B* **2002**, *106*, 10634−10640.
(11) Schaller, R. D.; Petruska, M. A.; Klimov, V. I. *J. Phys. Chem. B* **2003**, *107*, 13765−13768.
(12) Harbold, J. M.; Du, H.; Krauss, T. D.; Cho, K.-S.; Murray, C. B.; Wise, F. W. *Phys. Rev. B* **2005**, *72*, 195312.
(13) Klimov, V. I.; Mikhailovsky, A. A.; McBranch, D. W.; Leatherdale, C. A.; Bawendi, M. G.; *Science* **2000**, *287*, 1011−1013.
(14) Burda, C.; Chen, X.; Narayanan, R.; El-Sayed, M. A. *Chem. Rev.* **2005**, *105*, 1025−1102.
(15) Wundke, K.; Pötting, S.; Auxier, J.; Schülzgen, A.; Peyghambarian, N.; Borrelli, N. F. *Appl. Phys. Lett.* **2000**, *76*, 10−12.
(16) Patel, A. A.; Wu, F.; Zhang, J. Z.; Torres-Martinez, C. L.; Mehra, R. K.; Yang, Y.; Risbud, S. H. *J. Phys. Chem. B* **2000**, *104*, 11598−11605.
(17) Wu, F.; Yu, J. H.; Joo, J.; Hyeon, T.; Zhang, J. Z. *Opt. Mater.* **2007**, *29*, 858−866.
(18) Kang, I.; Wise, F. W. *J. Opt. Soc. Am. B* **1997**, *14*, 1632−1646.
(19) Ellingson, R. J.; Beard, M. C.; Johnson, J. C.; Yu, P.; Micic, O. I.; Nozik, A. J.; Shabaev, A.; Efros, A. L. *Nano Lett.* **2005**, *5*, 865−871.
(20) Sargent, E. H. *Adv. Mater.* **2005**, *17*, 515−522.
(21) See, for example, Leon-Garcia, A. *Probability and Random Processes for Electrical Engineering*; Addison-Wesley: Reading, MA, 1994; p 106.
(22) Coldren, L. A.; Corzine, S. W. *Diode Lasers and Photonic Integrated Circuits*; Wiley: New York, 1995.
(23) Klann, R.; Höfer, T.; Buhleier, R.; Elsaesser, T.; Tomm, J. W. *J. Appl. Phys.* **1995**, *77*, 277−286.
(24) Findlay, P. C.; Pidgeon, C. R.; Kotitschke, R.; Hollingworth, R.; Murdin, B. N.; Langerak, C. J. G. M.; van der Meer, A. F. G.; Ciesla, C. M.; Oswald, J.; Homer, A.; Springholz, G.; Bauer, G. *Phys. Rev. B* **1998**, *58*, 12908−12915.